Removal of Congo red dye by ultrafiltration composite membrane of PpPD/PVA on flat pozzolan/micronized phosphate ceramic support

Dounia Beqqour[a,*], Wiame Taanaoui[a], Mohamed Ouammou[a], Saad Alami Younssi[a], Jamal Bennazha[a], Jason A. Cody[b], M. El Rhazi[a]

[a]Laboratory of Materials, Membranes and Environment, Faculty of Sciences and Technologies Mohammedia, University Hassan II of Casablanca, Morocco, emails: dounia.beqqour-etu@etu.univh2c.ma (D. Beqqour), wiametaanaoui@gmail.com (W. Taanaoui), mouammou@yahoo.fr (M. Ouammou), alamiyounssisaad@yahoo.fr (S.A. Younssi), jbennazha@yahoo.fr (J. Bennazha), elrhazim@hotmail.com (M. El Rhazi)
[b]Department of Chemistry, Lake Forest College, 555 N. Sheridan Rd., Lake Forest, IL, USA, email: cody@mx.lakeforest.edu

ABSTRACT

A new composite ultrafiltration membrane made of poly(p-phenylenediamine) and poly(vinyl alcohol) as a selective layer on flat ceramic support fabricated from pozzolan and micronized phosphate was developed and characterized. The p-phenylenediamine was polymerized via a chemical route. The active layer was deposited on the flat support by dip-coating. The poly(p-phenylenediamine) and 10 wt.% of polyvinyl alcohol solution were used as the initial suspension. The composite membrane was kept for 24 h at 60°C. The developed membrane was characterized by Fourier transform infrared spectroscopy, scanning electron microscopy, energy-dispersive X-ray analysis, as well as water contact angle, permeability and filtration performance measurements. The obtained ultrafiltration membrane has a thickness of 4.1 μm, a water contact angle of 50°, a permeability of 12.20 L/h m² bar and pore size of 43 nm. In addition, the composite membrane presents good adhesion on the flat support. Furthermore, it was evaluated by tangential filtration of Congo red dye. The dye filtration was optimized by varying the operating conditions including the applied pressure (1–3 bar), the feed concentration (20–600 ppm) as well as the feed pH (4–10). Under the optimal conditions of Congo red filtration, the developed membrane achieved a rejection of 99.54% (at ΔP = 3 bar, C = 600 ppm and pH = 4).

Keywords: Poly(p-phenylenediamine); Poly(vinyl alcohol); Composite membrane; Pozzolan/micronized phosphate; Ultrafiltration; Congo red dye

1. Introduction

Through rapid developments in industrialization, climate change, population growth and over-consumption, sources of drinking water have been contaminated by human activities [1,2]. One of these major human activities is the textile industry. Indeed, this sector is one of the prime consumers and polluters of water. It generates large amounts of wastewater rich in dyes, salts, and reagents that have important potential impacts on the degradation of the environment [3]. The presence of organic dyes in wastewater is a significant contributor to water pollution [4]. Approximately 70% of dyes used in industry are azo dyes [5].

Congo red (CR) is one of the most hazardous organic dyes, due to its structural stability, its complicated aromatic structure as well as resistance to biodegradation [6]. CR properties combine to pose significant risks for the environment and human health, its discoloration and degradation is a major concern for the protection of the environment [7].

* Corresponding author.

To address this problem, water treatment techniques are required including coagulation, chlorination, ozonation, flotation, chemical oxidation, adsorption, reverse osmosis, ultrafiltration (UF) and nanofiltration [1,4]. Membrane filtration, particularly low-pressure UF is one of the most attractive and powerful treatment processes because it is a cost-effective and sustainable wastewater technology [8,9]. It offers great stability, easy operation, and high efficiency [10,11].

Although several studies explored the elaboration of ceramic membranes from industrial oxides such as silica, alumina, zirconia and titania, the approach is costly. As an alternative, there has been interested in using low-cost natural materials for membrane preparation [12–18]. Recently, many low-cost UF membranes were developed based on these materials [19–21]. Besides, plenty of research was oriented toward the development of UF composite membranes (CMs). The composite polymer-ceramic membranes are characterized by structural integrity, fouling resistance, and both high flux and selectivity [22]. Moreover, CMs prepared from polymers on low-cost ceramic supports attracted much interest. For instance, pozzolan was used as a support for both, the development of polypyrrole UF membrane for CR removal [23] and the preparation of polysulfone/polyetherimide UF layer for removal of methyl orange and acid orange 74 [24].

This paper presents the development of a new CM prepared by depositing an organic layer of poly(p-phenylenediamine) (PpPD) and poly(vinyl alcohol) (PVA) on a flat pozzolan ceramic support incorporated with micronized phosphate (Pz/MP). This support was selected for the preparation of the UF membrane because of its interesting attributes such as porosity (32.07%), permeability (1,732.50 L/h m^2 bar) and mechanical strength (15.69 MPa) as mentioned in our previous work [25].

The PpPD is brown–to–black and insoluble in water [26]. It was selected as an organic layer for its wide applications, particularly in water treatment [27,28]. PVA was selected for inclusion since it is an excellent biodegradable biopolymer. Because of its environmentally friendly properties, PVA has been widely used to fabricate PVA-based ceramic and polymeric membranes for various industrial applications [29,30].

The characteristics of these polymers (PpPD and PVA), as well as the Pz/MP support, will combine to enhance the performance of the developed PpPD/PVA membrane with respect to permeability and rejection. To evaluate the efficiency of the CM and to investigate the morphology as well as the hydrophobicity of the membrane surface,

a series of characterization techniques have been used: Fourier transform infrared spectroscopy (FTIR), scanning electron microscopy (SEM), energy-dispersive X-ray analysis (EDX) and water contact angle measurements (WCA). The evaluation of the membrane performance in terms of dye removal from aqueous solution was studied via tangential filtration using CR dye. Filtration performance is influenced basically by three parameters including the operating pressure, the feed concentration and the feed pH. This work also addressed the antifouling characteristics of the developed PpPD/PVA UF membrane.

2. Experimental

2.1. Materials

In order to elaborate the CM, the selective PpPD/PVA layer was deposited on a flat Pz/MP ceramic support that was prepared as previously described [25]. This support is characterized by a diameter of 37 mm, a thickness of 2.90 mm, a porosity of about 32.07%, a permeability of about 1,732.50 L/h m^2 bar and mechanical strength of 15.69 MPa.

The p-phenylenediamine (pPD) monomer and CR dye (35%) were purchased from Sigma-Aldrich. The properties of CR dye are summarized in Table 1. PVA (Rhodoviol 25/140) and ammonium persulfate (APS, 98%) were obtained from Prolabo and Loba Chemie, respectively. Hydrochloric acid (HCl, 37%) was obtained from VWR Chemicals.

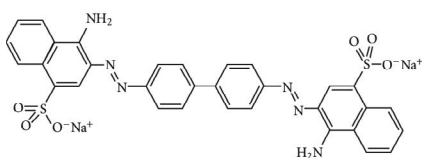### 2.2. Chemical polymerization of the pPD

To the pPD monomer (1 M), the oxidant APS was dissolved in HCl (0.5 M) and added dropwise under continuous stirring, then the solution was stirred for an additional 6 h in order to complete the polymerization. The obtained PpPD was recuperated, washed with distilled water and dried at 60°C.

2.3. Preparation of the PpPD/PVA membrane

Prior to any modification, the flat Pz/MP ceramic support was sonicated in water for 20 min to remove residual particles before drying overnight at 100°C. Next, the PpPD powder was added to a solution of PVA (10 wt.%) under constant magnetic stirring resulting in a mass ratio of PpPD/PVA of 0.47 [30].

Under atmospheric conditions, the support surface was coated by the PpPD/PVA suspension via dip-coating and left for 1 h. Then, it was dried for 24 h at 60°C [30]. The

Table 1
Characteristics of CR dye

Molecular formula	Chemical structure depiction	Molecular weight (g/mol)	Charge	Wavelength (λ_{max}, nm)
$C_{32}H_{22}N_6Na_2O_6S_2$		696.66	Anionic	499

resulting membrane was characterized and evaluated without any additional treatment or modification.

2.4. UF experiments

The effectiveness of the fabricated CM was measured by tangential filtration using a laboratory UF pilot described in Fig. 1. Briefly, it mainly contains a storage tank of 5 L, a membrane holder with an effective filtration area of 4.52 cm², manometers, circulation pump, air compressor and cooling system to maintain the feed solution at a constant temperature. The membrane permeability was measured by filtration of water at different operating pressures ranging from 1 to 3 bar at room temperature. Permeate flux J_w (L/h m²) and the permeability L_p (L/h m² bar) crossing the membrane are given by Eqs. (1) and (2) respectively:

$$J_w = \frac{V}{A \cdot t} \tag{1}$$

$$J_w = L_p \cdot \Delta P \tag{2}$$

where V (L) is the volume of permeate that crosses the specific surface A (m²) during interval time t (h) and ΔP is the operating pressure (bar).

To evaluate the performance of the PpPD/PVA membrane, a series of experiments on CR were carried out. The effect of different experimental parameters on filtration performance was studied. Parameters investigated included the operating pressure which varied from 1 to 3 bar, the feed concentration ranging from 20 to 600 ppm and the feed pH which was adjusted between 4 and 10 by adding HCl (2 M) and NaOH (2 M) solutions. All the effects were studied over 2 h of filtration.

The rejection factor R (%) was calculated by Eq. (3):

$$R = \left(1 - \frac{C_{\text{permeate}}}{C_{\text{feed}}}\right) \times 100 \tag{3}$$

where C_{permeate} and C_{feed} (ppm) are respectively the concentration of the permeate and the feed.

2.5. Antifouling study

The antifouling attributes of the membrane were investigated after 2 h of water filtration, and flux was measured (J_p, L/m² h) at the operating pressure of 3 bar. The antifouling capability of the membrane was characterized by calculating flux recovery ratio (FRR), total flux decline ratio (TFR), reversible flux decline ratio (RFR) and irreversible flux decline ratio (IFR) using the following equations [20].

$$\text{FRR} = \frac{J_{w1}}{J_{w0}} \times 100 \tag{4}$$

$$\text{TFR} = \left(1 - \frac{J_p}{J_{w0}}\right) \times 100 \tag{5}$$
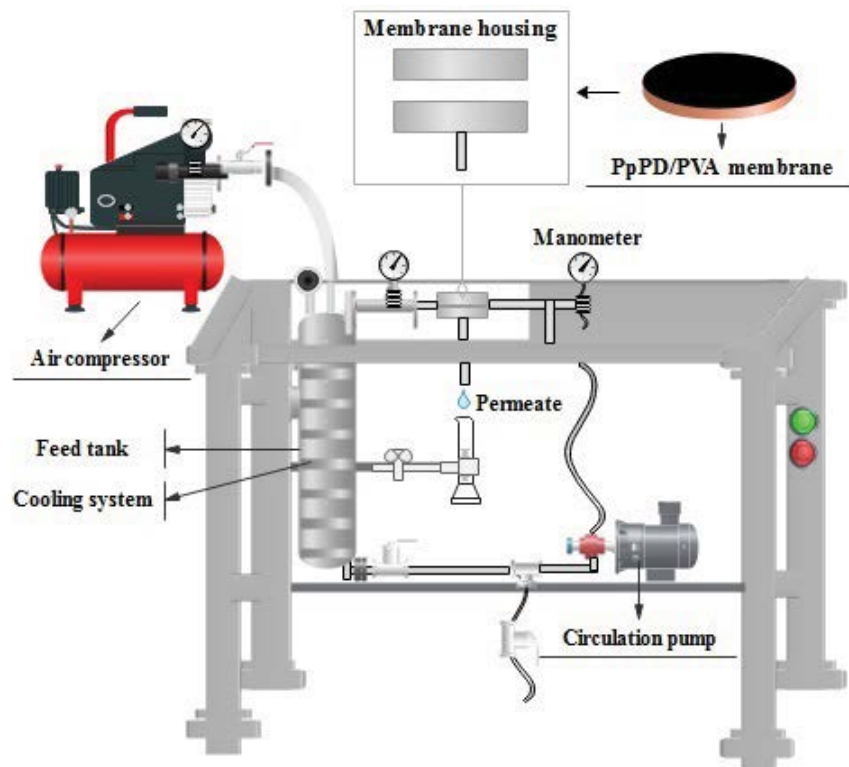

Fig. 1. Scheme of UF filtration pilot.

$$RFR = \frac{J_{w1} - J_p}{J_{w0}} \times 100 \qquad (6)$$

$$IFR = \frac{J_{w0} - J_{w1}}{J_{w0}} \times 100 \qquad (7)$$

where J_{w0} is the water permeate flux, J_p is the permeate flux of the PpPD/PVA membrane using CR dye at a concentration of 600 ppm. After cleaning and rinsing the membrane surface underwater, it was rinsed a second time for 1 h with water using the UF pilot under 3 bar. Then the permeate flux was measured a second time (J_{w1}) for 2 h.

2.6. Characterization

FTIR of the PpPD, PVA and the PpPD/PVA membrane layer (peeled off the flat ceramic support) was investigated using a Bruker Spectrometer (VERTEX 70). The top-view of the flat Pz/MP support and the PpPD/PVA membrane as well as the cross-section of the CM was characterized by SEM operating at 10 kV (FEI Company, Quanta 200). The elemental composition of the developed membrane was identified using the EDX detector on the SEM.

The average pore size was calculated using the extended Hagen–Poiseuille equation [31]:

$$d = 2\sqrt{8J_w \cdot \delta \cdot \frac{\tau}{\varepsilon} \cdot \frac{\Delta X}{\Delta P}} \qquad (8)$$

where d (m) is the pore diameter, J_w (m/s) is the water flux, δ (Pa·s) is the water viscosity, τ is the tortuosity factor (2.5 for sphere particle packing), ε (%) is the porosity of the membrane, ΔP (Pa) is the applied pressure, and ΔX (m) is the membrane thickness.

The WCA for the Pz/MP support and the PpPD/PVA membrane was measured using a Digidrop goniometer (GBX Instruments), then the solution pH was measured using a pH meter (METTLER TOLEDO SevenCompact pH/Ion). UV-Vis spectrophotometry (JASCO V-730 Spectrophotometer) was employed to measure the CR concentration before and after filtration at a maximum absorbance wavelength of 499 nm using quartz cells. The determination of the point of zero charge (PZC) of PpPD/PVA membrane was ensured by the solid addition method as described elsewhere [32].

3. Results and discussion

3.1. Characterization of the PpPD/PVA membrane

3.1.1. FTIR analysis

The FTIR spectra of the PVA, PpPD, and PpPD/PVA layers are shown in Fig. 2. For PVA, the highest band intensity in the region of 3,280 cm^{-1} is attributed to the O–H stretching vibration of the hydroxyl group [33,34]. The peaks at 2,917 and 1,718 cm^{-1} are due to CH$_2$ asymmetric stretching vibration [34] and the C=O vibration [35], respectively. The peak at 1,425 cm^{-1} is linked to C–H bending vibration of CH$_2$ [30,34] while the peak at 1,324 cm^{-1} is attributed to

C–H deformation vibration [33]. The peak at 1,081 cm^{-1}, corresponds to C–O stretching of acetyl groups [34] whereas the peak at 916 cm^{-1} is due to CH$_2$ rocking [34], and the last peak at 839 cm^{-1} is assigned to C–C stretching [30,33].

For the PpPD, the band at 3,240 is due to the stretching vibrations of the N–H group [36]. The peak at 1,576 and 1,504 cm^{-1} can be attributed to stretching deformations of quinone and phenazine rings, respectively [37,38]. For the peak located at 1,407 cm^{-1}, it corresponds to the C–N–C stretching vibration of benzenoid units [38]. The peaks at 1,346 and 1,286 cm^{-1} can be due to the C–N stretching vibration in quinoid imine (–C=N–) and benzenoid units C–N, respectively [39]. The peak at 819 cm^{-1} can be ascribed to the C–H out-of-plane bending vibration of the 1,2,4,5-tetra-substituted benzene ring [39].

In the spectrum of the PpPD/PVA membrane layer, peaks correspond for both PVA and PpPD and some of these peaks slightly shifted towards shorter wavenumber.

3.1.2. WCA measurement

The surface wettability measurements of both Pz/MP support and the PpPD/PVA membrane surface were examined via the WCA technique and results are depicted in Fig. 3. For the Pz/MP ceramic support, the drop of water
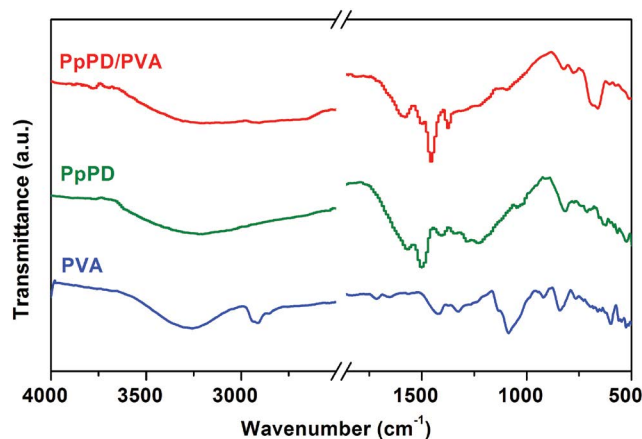

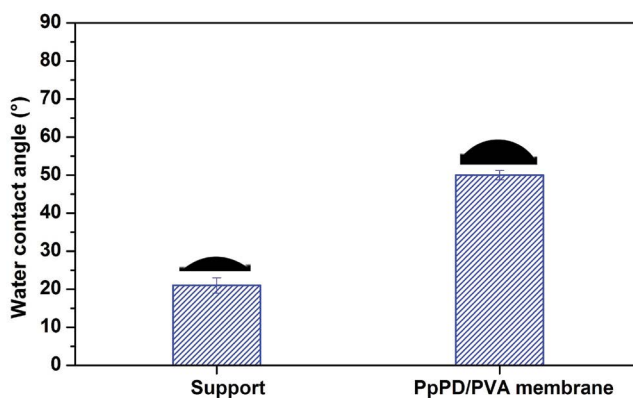Fig. 2. FTIR spectra of PVA, PpPD and PpPD/PVA membrane layer.

Fig. 3. WCA of Pz/MP support and PpPD/PVA membrane.

permeates almost immediately on the support surface. The rather hydrophilic character of this surface was confirmed by the obtained value of WCA which is equal to 21°. This deduction is coherent with the porous morphology of the flat ceramic support. For the PpPD/PVA membrane, the WCA is about 50° which means that the membrane surface becomes less hydrophilic compared to the bare Pz/MP support.

3.1.3. Permeability

Results of permeate flux (of water) for the Pz/MP support and the PpPD/PVA membrane vs. operating pressure ranging from 1 to 3 bar are displayed in Fig. 4. The relationships between flux and pressure in an operating pressure range from 1 to 3 are both clearly linear. The slopes give permeability values equal to 1,732.50 L/h m^2 bar for the Pz/MP support (Fig. 4a) and 12.20 L/h m^2 bar for the PpPD/PVA membrane (Fig. 4b). Not surprisingly, the permeability was reduced by a factor of 142 after deposition of the PpPD/PVA layer on the Pz/MP support.

3.1.4. SEM observation

Fig. 5 illustrates the SEM images of the top-views for both the flat Pz/MP support and the PpPD/PVA membrane, as well as the cross-section of the developed membrane. The morphology of the flat support is microporous with
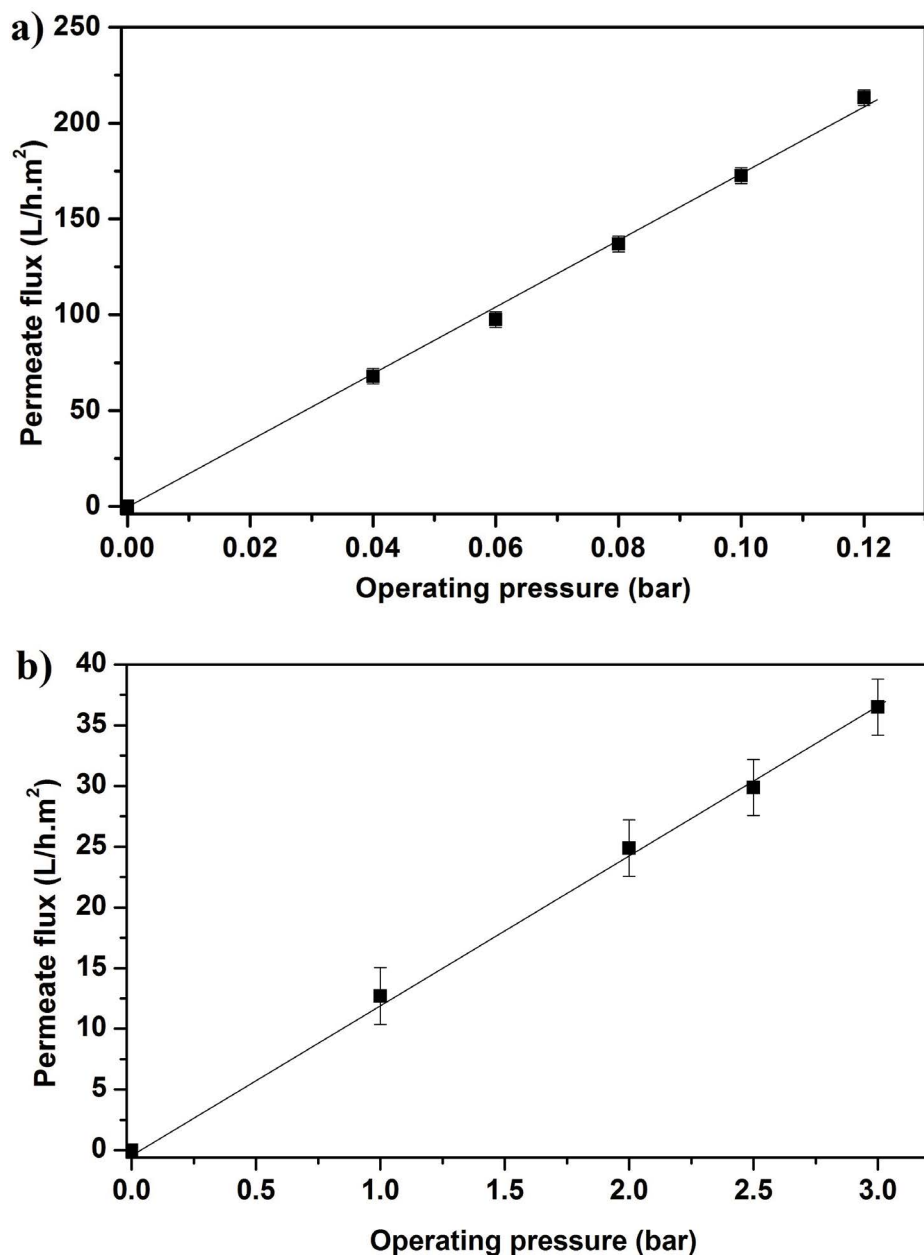

Fig. 4. Permeate flux as a function of operating pressure of (a) Pz/MP support and (b) PpPD/PVA membrane.

an irregular and heterogeneous distribution of particles. The developed membrane, in contrast, has a homogenous surface with a granular morphology due to the PpPD particles [37]. The cross-section of the PpPD/PVA membrane is revealing a rather uniform layer deposition of 4.1 μm in thickness (determined from an average of four measured values) on the Pz/MP support.

3.1.5. EDX analysis

The EDX spectrum of the PpPD/PVA membrane is shown in Fig. 6. Intense peaks of carbon (C), oxygen (O) and nitrogen (N) are observed with a weight percentages of 40.41, 41.60 and 13.31 wt.%, respectively. Recall that the PpPD is a compound composed of C and N, and the PVA
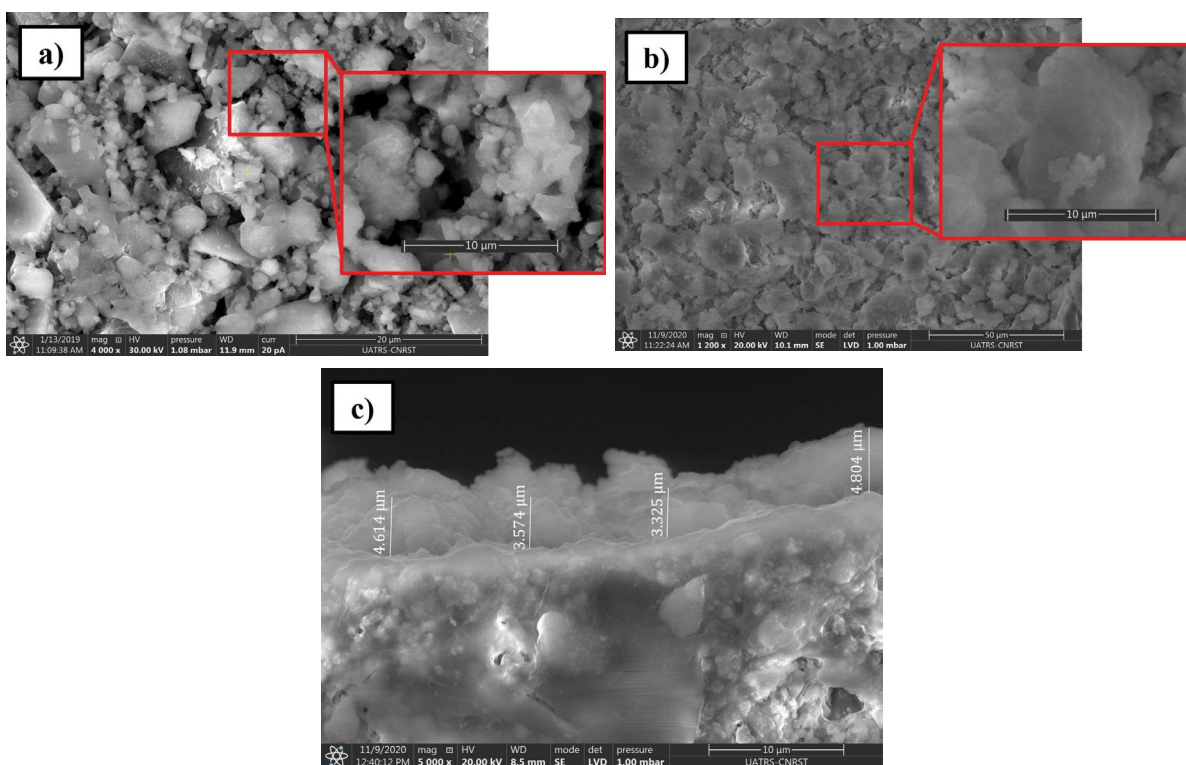

Fig. 5. SEM micrographs of top-view of the Pz/MP support (a), the PpPD/PVA membrane (b), and cross-section (c) of the CM.

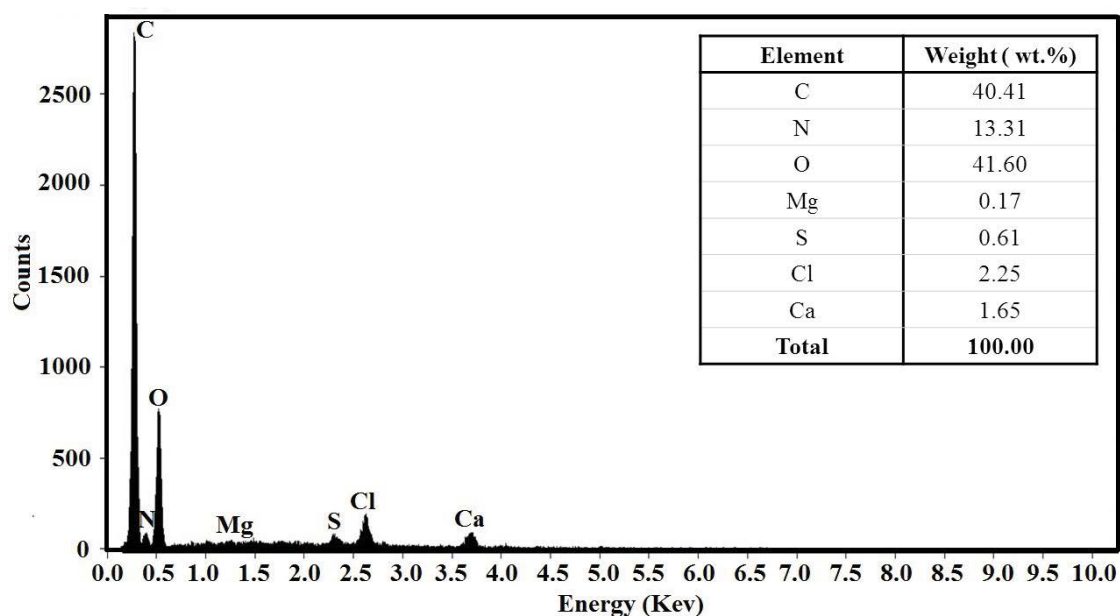| Element	Weight (wt.%)
C	40.41
N	13.31
O	41.60
Mg	0.17
S	0.61
Cl	2.25
Ca	1.65
Total	**100.00**

Fig. 6. EDX spectrum of PpPD/PVA membrane.

contains C and O. Additional O might be detected from the underlying Pz/MP support. Moreover, the presence of chlorine (Cl) and the trace amounts of calcium (Ca), sulfur (S) and magnesium (Mg) are attributed to the chemical composition of the flat ceramic support.

These findings indicate that PpPD and PVA contain the intended elemental compositions and are deposited as a layer on the Pz/MP support.

3.1.6. Pore size

The pore size of the PpPD/PVA membrane was calculated and found to be 43 nm. This means that the developed membrane could be used for UF applications such as the removal of organic soluble dyes.

3.2. UF experiments

In this section, the efficiency of the PpPD/PVA membrane was performed by evaluating the removal of CR dye. The effect of operating pressure, feed concentration and pH were studied and optimized.

3.2.1. Effect of operating pressure

The effect of operating pressure (from 1 to 3 bar) on the permeate flux and the removal of CR dye for the UF membrane was studied as shown in Fig. 7. This effect was evaluated during 2 h of dye filtration at a constant feed concentration of 20 ppm and a solution pH around 6.45 which is approximately the pH_{PZC} determined experimentally of the membrane ($pH_{PZC} = 6.45$).
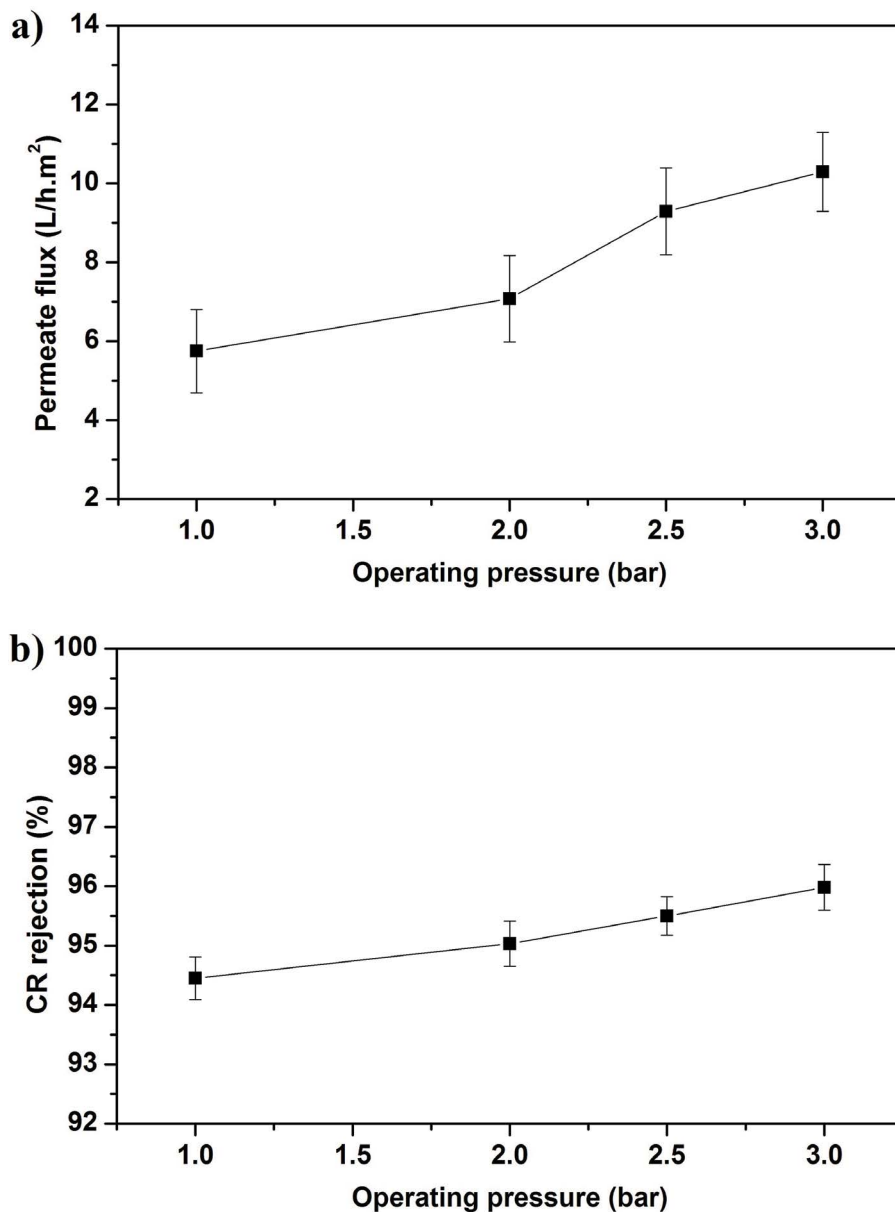

Fig. 7. CR permeate flux (a) and rejection (b) as a function of operating pressure at $C = 20$ ppm and pH = 6 for 2 h of filtration.

Increasing the operating pressure from 1 to 3 bar gives a corresponding increase in the permeate flux from 5.75 to 10.29 L/h m² after 2 h of dye filtration as depicted in Fig. 7a. This is due to the increase in driving force across the membrane. It is remarkable that the permeate flux is less important than the permeate flux of water (Fig. 4b). The difference in fluxes can be explained by a multitude of phenomena such as the adsorption of dyes particles on the effective filtration area and in pores [40].

By increasing the operating pressure from 1 to 3 bar (Fig. 7b), the CR rejection increases from 94.45 to 95.98% after 2 h of filtration. It is clear that a higher operating pressure gives a higher rejection, consistent with other studies [30]. This result agrees with the classical (Spiegler–Kedem) convection/diffusion model for solute transport [23,30].

3.2.2. Effect of feed concentration

The variation of the flux and the rejection of CR dye as a function of feed concentration through the PpPD/PVA membrane is illustrated in Fig. 8. To investigate the effect of the feed concentration, this last was varied from 20 to 600 ppm while the pressure and the pH remain constant at values of 3 and 6.45 (pH_{PZC} = 6.45), respectively. Generally, higher feed concentration results in lower permeate flux [41]. As anticipated, the permeate flux decreases from 10.29 to 6.64 L/h m² when the feed concentration increases from 20 to 600 ppm as shown in Fig. 8a. This might be due to membrane surface settlement by the CR particles, or insertion into the pores, therefore increasing membrane fouling that leads to a reduction in permeate flux [40]. This result can be linked to the increase in concentration polarization.

According to the rejection results displayed in Fig. 8b, increasing the concentration causes a slight increase in the rejection after 2 h of filtration: at 20 ppm the rejection was 95.98% and increases to 97.22% when the feed concentration is 600 ppm. This variation could be explained by the formation of a polarization layer following an accumulation of anionic CR dye molecules on the surface area of the PpPD/PVA membrane. This second layer acts as a second membrane [42]. Note that the only possible mode of transport through this polarization layer is likely to be diffusion [43]. The same deductions were found in other studies [19,44,45].
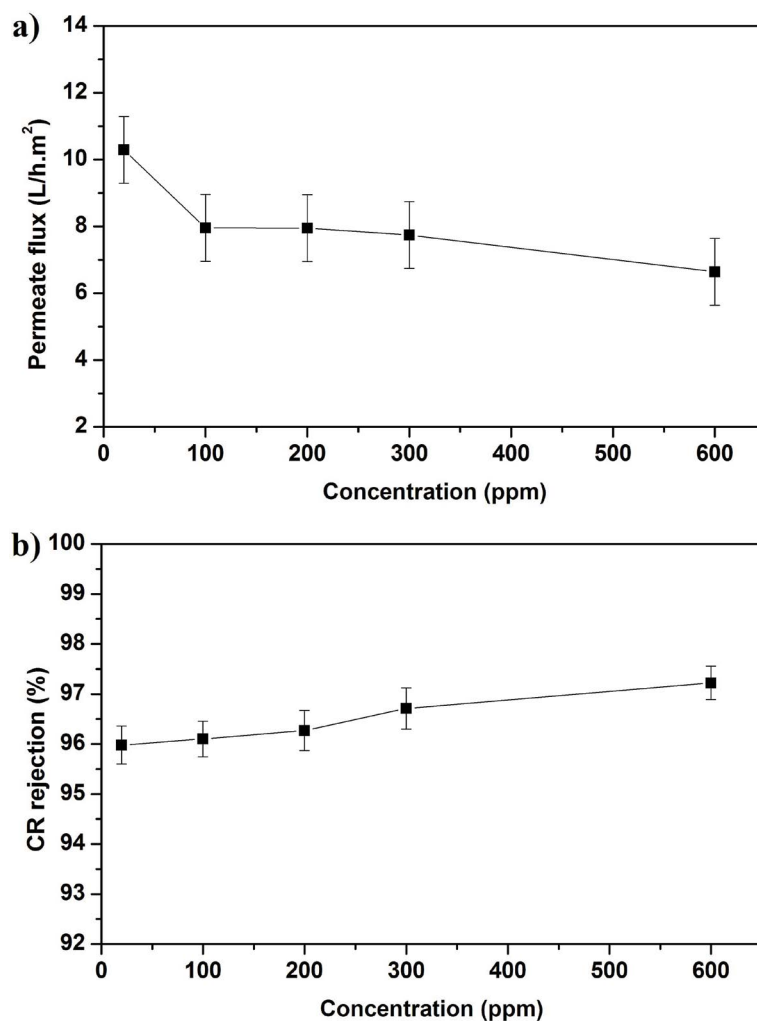

Fig. 8. CR permeate flux (a) and rejection (b) as a function of feed concentration at ΔP = 3 bar and pH = 6 for 2 h of filtration.

3.2.3. Effect of feed pH

The performance of the PpPD/PVA membrane not only depends on operating pressure and the feed concentration but also depends on feed pH. Since the pH determines the charge of CR dye molecules and influences the membrane, its effect is an important factor in CR removal [46]. The feed pH effect range of 4–10 on the permeate flux and the removal of CR dye was assessed as depicted in Fig. 9. This effect was evaluated by filtration of aqueous dye solutions under a constant feed concentration of 600 ppm and an operating pressure of 3 bar over 2 h of filtration.

Fig. 9a shows the permeate flux of the membrane with different pH. It remains nearly constant across the range, increasing from 6.63 to only 6.68 L/h m^2 bar, whereas Fig. 9b shows that the rejection of the CR decreases from 99.54% to 93.2% with an increase in pH. The minimum permeate flux and the maximum CR rejection were reached in an acidic medium (pH = 4). Under this condition, the color of CR is dark blue and dye sediments occur [47].

Furthermore, the protonation of the CR sulfonated acid groups reduces both the polarity and solubility of CR, causing dye aggregation and precipitation [48]. As a result, the permeate flux slightly decreases due to dye aggregation and precipitation on the effective surface of the UF membrane leading to membrane fouling. For the rejection, the phenomenon of polarization may be responsible for its increase in the acidic medium. The point of zero charge (pH$_{PZC}$) of the PpPD/PVA membrane is about 6.45, meaning that the membrane surface has a positive charge at pH below 6.45 and it is negative above this pH value.

At low pH values, the positive electrostatic charges on the surface of the membrane attract the negatively charged ions of CR dye, forming a polarization layer [23,30]. The resulting negatively charged layer of CR particles on the surface results in additional repulsion of negative CR molecules in solution. However, in the basic medium, the permeate flux is greater, but the rejection declines with increasing solution pH. The electrostatic attractions became weaker between dye particles and the PpPD/PVA membrane
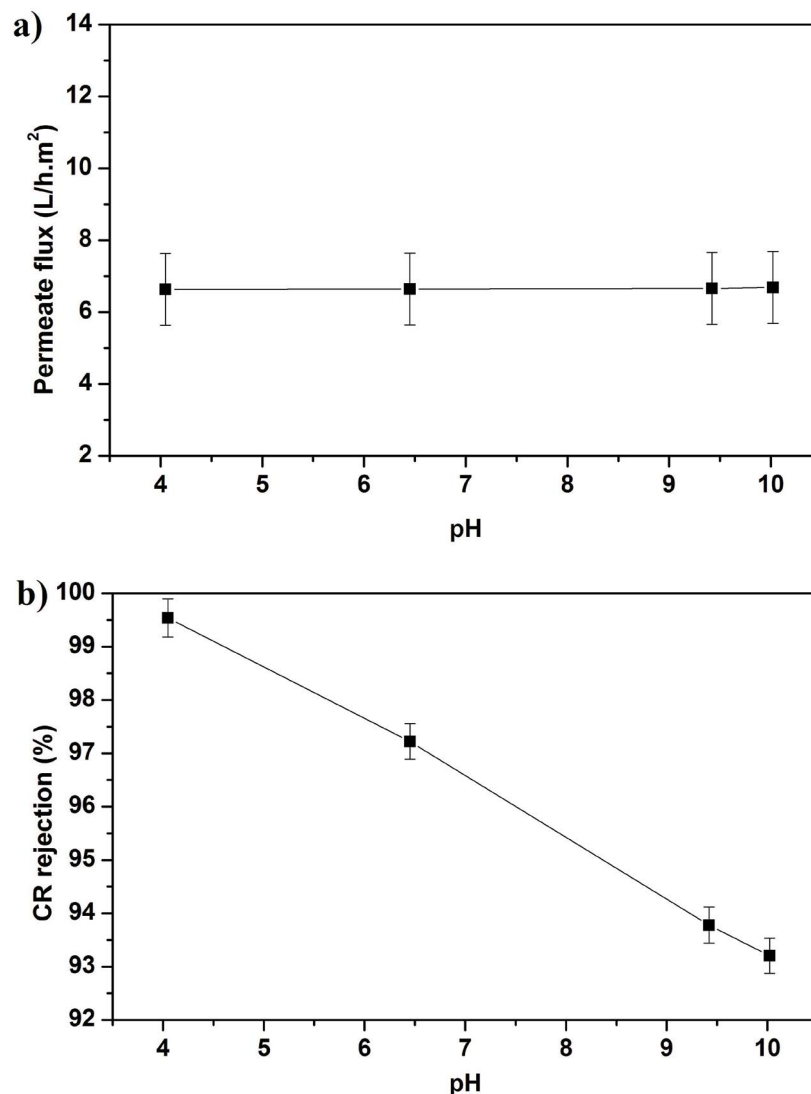

Fig. 9. CR permeate flux (a) and rejection (b) as a function of feed pH at ΔP = 3 bar and C = 600 ppm for 2 h of filtration.
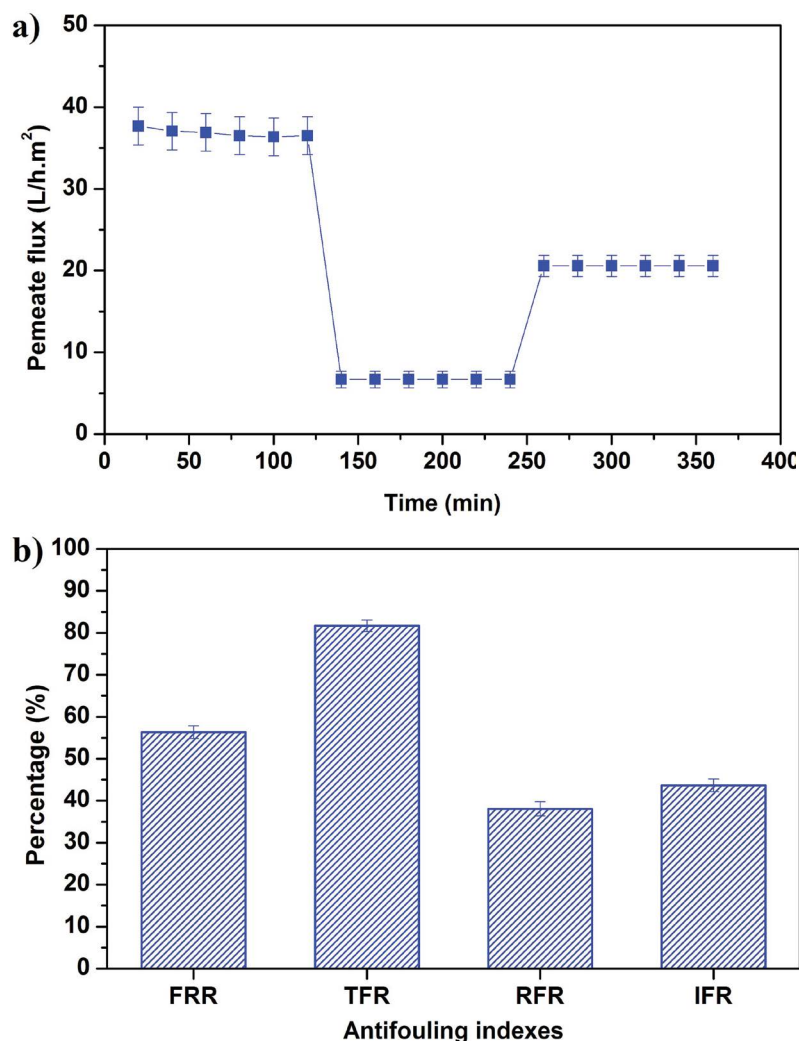
Fig. 10. Permeate flux during filtration experiments (a) and antifouling parameters of PpPD/PVA membrane (b).

surface which leads to a reduction in CR rejection rate. Apparently, the surface layer of CR molecules on the membrane at low pH is more negative (greater rejection) than the negative surface of the membrane at high pH (above pH_{PZC}).

3.3. Antifouling study

The fouling of the membrane is the most significant problem encountered in filtration and likely occurs by the accumulation of molecules on the surface and in the pores. Fouling negatively affects UF membrane performance, shortens the lifetime of membranes, increases the cost of maintenance and reduces the water penetration flux [5]. Although membrane fouling can be reduced, it is inevitable [49]. The antifouling properties of the PpPD/PVA membrane used for CR removal were studied by determining four fouling parameters (FRR, TFR, RFR and IFR). Note that all permeate fluxes were normalized to the initial water flux J_{w0}.

Fig. 10 shows the water permeate and CR solution flux as well as the antifouling properties of the PpPD/PVA membrane. By comparing the permeate flux (Fig. 10a) of water (time = 0–120 min), of CR solution (pH = 10 and

C = 600 ppm, time = 120–240 min) and then of water again (time = 240–360 min) the decrease and partial recovery of the flux are obvious. The proposed polarization layer is likely responsible for the drop; good restoration was obtained after physical cleaning and rinsing of the surface. As shown in Fig. 10b, the permeate flux of the membrane recovers to (FRR = 56.36%) with a TFR value of 81.70%. The increase in this rate is related to the formation of a concentrated polarization layer on the membrane. These measurements are consistent with the results reported in the previous Section 3.2.2. The fouling caused by the polarization layer is expressed by the RFR (38.06%), indicating the amount of fouling that might be removed by membrane rinsing. In contrast, the pore blockage is calculated by the IFR (43.63%) and is irreversible without chemical cleaning [50].

4. Conclusion

In this work, PpPD and PVA were effectively used for the development of a new UF membrane prepared via dip-coating on flat ceramic support made from pozzolan and micronized phosphate. The polymerization of pPD

and the co-deposited membrane selective layer (PpPD/PVA) was confirmed by FTIR analysis. According to SEM images, the morphology of the developed membrane is uniform and does not exhibit any defects and shows good adherence to the support. The fabricated membrane has a WCA of 50°, a permeability of 12.20 L/h m² bar, a pore size of 43 nm and an average thickness of 4.1 μm. The PpPD/PVA membrane removed CR dye from aqueous solutions under various operating pressures (1–3 bar), feed concentrations (20– 00 ppm) and feed pH values (4–10). Under the optimal conditions, the rejection of the UF membrane reached 99.54% in an acidic medium (pH = 4), at 600 ppm of CR and operating pressure of 3 bar. Furthermore, the developed UF membrane presents attractive antifouling properties.

According to these promising results, the developed UF membrane in this paper could be used as an alternative for dye removal as well as employed for wastewater treatment particularly generated from textile industries.

Acknowledgment

References

[1] S. Kim, K.H. Chu, Y.A.J. Al-Hamadani, C.M. Park, M. Jang, D.-H. Kim, M. Yu, J. Heo, Y. Yoon, Removal of contaminants of emerging concern by membranes in water and wastewater: a review, Chem. Eng. J., 335 (2018) 896–914.

[2] J. Shen, H. Ruan, L. Wu, C. Gao, Preparation and characterization of PES–SiO₂ organic–inorganic composite ultrafiltration membrane for raw water pretreatment, Chem. Eng. J., 168 (2011) 1272–1278.

[3] J. Babu, Z.V.P. Murthy, Treatment of textile dyes containing wastewaters with PES/ PVA thin film composite nanofiltration membranes, Sep. Purif. Technol., 183 (2017) 66–72.

[4] S. Chatterjee, N. Guha, S. Krishnan, A.K. Singh, P. Mathur, D.K. Rai, Selective and recyclable Congo red dye adsorption by spherical Fe₃O₄ nanoparticles functionalized with 1,2,4,5-benzenetetracarboxylic acid, Sci. Rep., 10 (2020) 1–11.

[5] F. Mehrjo, A. Pourkhabbaz, A. Shahbazi, PMO synthesized and functionalized by p-phenylenediamine as new nanofiller in PES-nanofiltration membrane matrix for efficient treatment of organic dye, heavy metal, and salts from wastewater, Chemosphere, 263 (2021) 1–12.

[6] M.K. Purkait, A. Maiti, S. DasGupta, S. De, Removal of Congo red using activated carbon and its regeneration, J. Hazard. Mater., 145 (2007) 287–295.

[7] L.A. Huda Alhassani, Efficient aerobic degradation of various azo dyes by a *Sphingomonas* sp. isolated from petroleum sludge, J. Biorem. Biodegrad., 5 (2014) 1–10.

[8] Z. Chu, K. Chen, C. Xiao, H. Ling, Z. Hu, Performance improvement of polyethersulfone ultrafiltration membrane containing variform inorganic nano-additives, Polymer, 188 (2020) 1–11.

[9] W. Zhang, W. Cheng, E. Ziemann, A. Be'er, X. Lu, M. Elimelech, R. Bernstein, Functionalization of ultrafiltration membrane with polyampholyte hydrogel and graphene oxide to achieve dual antifouling and antibacterial properties, J. Membr. Sci., 565 (2018) 293–302.

[10] H. Isawi, Development of thin-film composite membranes via radical grafting with methacrylic acid/ZnO doped TiO₂ nanocomposites, React. Funct. Polym., 131 (2018) 400–413.

[11] W. Xu, X. Sun, M. Huang, X. Pan, X. Huang, H. Zhuang, Novel covalent organic framework/PVDF ultrafiltration membranes with antifouling and lead removal performance, J. Environ. Manage., 269 (2020) 1–7.

[12] B. Achiou, H. Elomari, M. Ouammou, A. Albizane, J. Bennazha, S.A. Younssi, I.E.E. Amrani, A. Aaddane, Elaboration and characterization of flat ceramic microfiltration membrane made from natural Moroccan pozzolan (Central Middle Atlas), J. Mater. Environ. Sci., 7 (2016) 196–204.

[13] H. Elomari, B. Achiou, M. Ouammou, A. Albizane, J. Bennazha, S. Alami Younssi, I. Elamrani, Elaboration and characterization of flat membrane supports from Moroccan clays. Application for the treatment of wastewater, Desal. Water Treat., 57 (2016) 20298–20306.

[14] A. Bouazizi, S. Saja, B. Achiou, M. Ouammou, J.I. Calvo, A. Aaddane, S.A. Younssi, Elaboration and characterization of a new flat ceramic MF membrane made from natural Moroccan bentonite. Application to treatment of industrial wastewater, Appl. Clay Sci., 132–133 (2016) 33–40.

[15] S. Saja, A. Bouazizi, B. Achiou, M. Ouammou, A. Albizane, J. Bennazha, S.A. Younssi, Elaboration and characterization of low-cost ceramic membrane made from natural Moroccan perlite for treatment of industrial wastewater, J. Environ. Chem. Eng., 6 (2018) 451–458.

[16] O. Samhari, S. Alami Younssi, M. Rabiller-Baudry, P. Loulergue, M. Bouhria, B. Achiou, M. Ouammou, Fabrication of flat ceramic microfiltration membrane from natural kaolinite for seawater pretreatment for desalination and wastewater clarification, Desal. Water Treat., 194 (2020) 59–68.

[17] A. Belgada, B. Achiou, S. Alami Younssi, F.Z. Charik, M. Ouammou, J.A. Cody, R. Benhida, K. Khaless, Low-cost ceramic microfiltration membrane made from natural phosphate for pretreatment of raw seawater for desalination, J. Eur. Ceram. Soc., 41 (2021) 1613–1621.

[18] B. Achiou, H. Elomari, A. Bouazizi, A. Karim, M. Ouammou, A. Albizane, J. Bennazha, S. Alami Younssi, I.E. El Amrani, Manufacturing of tubular ceramic microfiltration membrane based on natural pozzolan for pretreatment of seawater desalination, Desalination, 419 (2017) 181–187.

[19] A. Bouazizi, M. Breida, B. Achiou, M. Ouammou, J.I. Calvo, A. Aaddane, S.A. Younssi, Removal of dyes by a new nano-TiO₂ ultrafiltration membrane deposited on low-cost support prepared from natural Moroccan bentonite, Appl. Clay Sci., 149 (2017) 127–135.

[20] H. Ouaddari, A. Karim, B. Achiou, S. Saja, A. Aaddane, J. Bennazha, I. El Amrani El Hassani, M. Ouammou, A. Albizane, New low-cost ultrafiltration membrane made from purified natural clays for direct Red 80 dye removal, J. Environ. Chem. Eng., 7 (2019) 1–10.

[21] S. Saja, A. Bouazizi, B. Achiou, H. Ouaddari, A. Karim, M. Ouammou, A. Aaddane, J. Bennazha, S. Alami Younssi, Fabrication of low-cost ceramic ultrafiltration membrane made from bentonite clay and its application for soluble dyes removal, J. Eur. Ceram. Soc., 40 (2020) 2453–2462.

[22] M. Changmai, M.K. Purkait, Detailed study of temperature-responsive composite membranes prepared by dip coating poly(2-ethyl-2-oxazoline) onto a ceramic membrane, Ceram. Int., 44 (2018) 959–968.

[23] G. Derouich, S. Alami Younssi, J. Bennazha, J.A. Cody, M. Ouammou, M. El Rhazi, Development of low-cost polypyrrole/sintered pozzolan ultrafiltration membrane and its highly efficient performance for Congo red dye removal, J. Environ. Chem. Eng., 8 (2020) 1–10.

[24] S. Benkhaya, B. Achiou, M. Ouammou, J. Bennazha, S. Alami Younssi, S. M'rabet, A. El Harfi, Preparation of low-cost composite membrane made of polysulfone/polyetherimide ultrafiltration layer and ceramic pozzolan support for dyes removal, Mater. Today Commun., 19 (2019) 212–219.

[25] D. Beqqour, B. Achiou, A. Bouazizi, H. Ouaddari, H. Elomari, M. Ouammou, J. Bennazha, S. Alami Younssi, Enhancement

of microfiltration performances of pozzolan membrane by incorporation of micronized phosphate and its application for industrial wastewater treatment, J. Environ. Chem. Eng., 7 (2019) 1–10.

[26] J. Stejskal, Polymers of phenylenediamines, Prog. Polym. Sci., 41 (2015) 1–31.

[27] S. Yang, D. Liu, F. Liao, T. Guo, Z. Wu, T. Zhang, Synthesis, characterization, morphology control of poly (p-phenylenediamine)-Fe$_3$O$_4$ magnetic micro-composite and their application for the removal of Cr$_2$O$_7^{2-}$ from water, Synth. Met., 162 (2012) 2329–2336.

[28] Y.-L. Min, T. Wang, Y.-G. Zhang, Y.-C. Chen, The synthesis of poly(p-phenylenediamine) microstructures without oxidant and their effective adsorption of lead ions, J. Mater. Chem., 21 (2011) 6683–6689.

[29] Q. Dong, J. Liu, C. Yao, G. Shao, Poly(vinyl alcohol)-based polymeric membrane: preparation and tensile properties, J. Appl. Polym. Sci., 122 (2011) 1350–1357.

[30] D. Beqqour, G. Derouich, W. Taanaoui, A. Essate, M. Ouammou, S. Alami Younssi, J. Bennazha, J.A. Cody, M. El Rhazi, Development of composite ultrafiltration membrane made of PmPD/ PVA layer deposited on ceramic pozzolan/micronized phosphate support and its application for Congo red dye removal, Desal. Water Treat., (2021) (in Press).

[31] H. Elomari, B. Achiou, D. Beqqour, K. Khaless, R. Beniazza, M. Ouammou, A. Aaddane, S. Alami Younssi, R. Benhida, Preparation and characterization of low-cost zirconia/clay membrane for removal of acid orange 74 dye, Mater. Today:. Proc., (2021) (in Press).

[32] N. Fayoud, S. Tahiri, S. Alami Younssi, A. Albizane, D. Gallart-Mateu, M.L. Cervera, M. de la Guardia, Kinetic, isotherm and thermodynamic studies of the adsorption of methylene blue dye onto agro-based cellulosic materials, Desal. Water Treat., 57 (2016) 16611–16625.

[33] A. Kharazmi, N. Faraji, R. Mat Hussin, E. Saion, W.M.M. Yunus, K. Behzad, Structural, optical, opto-thermal and thermal properties of ZnS–PVA nanofluids synthesized through a radiolytic approach, Beilstein J. Nanotechnol., 6 (2015) 529–536.

[34] N.V. Bhat, M.M. Nate, M.B. Kurup, V.A. Bambole, S. Sabharwal, Effect of γ-radiation on the structure and morphology of polyvinyl alcohol films, Nucl. Instrum. Methods Phys. Res., Sect. B, 237 (2005) 585–592.

[35] Y. Chen, S. Xu, S. Han, S. Chu, L. Yang, C. Jiang, Reusable and removable PmPD/ PVA membrane for effective Cr(vi) adsorption and reduction, New J. Chem., 43 (2019) 5039–5046.

[36] T. Zhang, S. Yang, J. Sun, X. Li, L. He, S. Yan, X. Kang, C. Hu, F. Liao, Poly(p-phenylenediamine) fluorescent nanosphere: a ultra-sensitive fluorescent probe for caffeine, Synth. Met., 181 (2013) 86–91.

[37] T. Li, C. Yuan, Y. Zhao, Q. Chen, M. Wei, Y. Wang, Synthesis, characterization, and properties of aniline-p-phenylenediamine copolymers, High Perform. Polym., 25 (2013) 348–353.

[38] S. Archana, R. Jaya Shanthi, Synthesis and characterization of poly(p-phenylenediamine) in the presence of sodium dodecyl sulfate, Res. J. Chem. Sci., 4 (2014) 60–67.

[39] J. Jaidev, S. Ramaprabhu, Poly(p-phenylenediamine)/graphene nanocomposites for supercapacitor applications, J. Mater. Chem., 22 (2012) 18775–18783.

[40] R.V. Kumar, A.K. Ghoshal, G. Pugazhenthi, Fabrication of zirconia composite membrane by in-situ hydrothermal technique and its application in separation of methyl orange, Ecotoxicol. Environ. Saf., 121 (2015) 73–79.

[41] Y. He, G. Li, H. Wang, J. Zhao, H. Su, Q. Huang, Effect of operating conditions on separation performance of reactive dye solution with membrane process, J. Membr. Sci., 321 (2008) 183–189.

[42] A. Bouazizi, M. Breida, A. Karim, B. Achiou, M. Ouammou, J.I. Calvo, A. Aaddane, K. Khiat, S.A. Younssi, Development of a new TiO$_2$ ultrafiltration membrane on flat ceramic support made from natural bentonite and micronized phosphate and applied for dye removal, Ceram. Int., 43 (2017) 1479–1487.

[43] S.M.K. Sadr, D.P. Saroj, Chapter 14 – Membrane Technologies for Municipal Wastewater Treatment, A. Basile, A. Cassano, N.K. Rastogi, Eds., Advances in Membrane Technologies for Water Treatment: Materials, Processes and Applications, Woodhead Publishing Series in Energy, Elsevier, 2015, pp. 443–463.

[44] M. Jiang, K. Ye, J. Lin, X. Zhang, W. Ye, S. Zhao, B. van der Bruggen, Effective dye purification using tight ceramic ultrafiltration membrane, J. Membr. Sci., 566 (2018) 151–160.

[45] J. Lin, W. Ye, M.-C. Baltaru, Y.P. Tang, N.J. Bernstein, P. Gao, S. Balta, M. Vlad, A. Volodin, A. Sotto, P. Luis, A.L. Zydney, B. van der Bruggen, Tight ultrafiltration membranes for enhanced separation of dyes and Na$_2$SO$_4$ during textile wastewater treatment, J. Membr. Sci., 514 (2016) 217–228.

[46] N.H.H. Hairom, A.W. Mohammad, A.A.H. Kadhum, Nanofiltration of hazardous Congo red dye: Performance and flux decline analysis, J. Water Process Eng., 4 (2014) 99–106.

[47] C. Liu, H. Mao, J. Zheng, S. Zhang, Tight ultrafiltration membrane: preparation and characterization of thermally resistant carboxylated cardo poly(arylene ether ketone)s (PAEK-COOH) tight ultrafiltration membrane for dye removal, J. Membr. Sci., 530 (2017) 1–10.

[48] C. Yang, W. Xu, Y. Nan, Y. Wang, Y. Hu, C. Gao, X. Chen, Fabrication and characterization of a high-performance polyimide ultrafiltration membrane for dye removal, J. Colloid Interface Sci., 562 (2020) 589–597.

[49] N. Nikooe, E. Saljoughi, Preparation and characterization of novel PVDF nanofiltration membranes with hydrophilic property for filtration of dye aqueous solution, Appl. Surf. Sci., 413 (2017) 41–49.

[50] C. Lavanya, K. Soontarapa, M.S. Jyothi, R. Geetha Balakrishna, Environmental friendly and cost effective caramel for Congo red removal, high flux, and fouling resistance of polysulfone membranes, Sep. Purif. Technol., 211 (2019) 348–358.